Winter December, 2006

Guiding of Laser Beams in Plasmas by Radiation Cascade Compression

Serguei Y. Kalmykov
Gennady Shvets

Guiding of Laser Beams in Plasmas by Radiation Cascade Compression

Serguei Kalmykov and Gennady Shvets

Department of Physics and Institute for Fusion Studies,
The University of Texas at Austin, Austin, Texas 78712

Abstract. The near-resonant beatwave excitation of an electron plasma wave (EPW) can be employed for generating trains of few-fs electromagnetic pulses in rarefied plasmas. The EPW produces a co-moving index grating that induces a laser phase modulation at the beat frequency. Consequently, the cascade of sidebands red- and blue-shifted from the fundamental by integer multiples of the beat frequency is generated in the laser spectrum. When the beat frequency is lower than the electron plasma frequency, the phase chirp enables laser beatnote compression by the group velocity dispersion [S. Kalmykov and G. Shvets, Phys. Rev. E **73**, 046403 (2006)]. In the 3D cylindrical geometry, the frequency-downshifted EPW not only modulates the laser frequency, but also causes the pulse to self-focus [P. Gibbon, Phys. Fluids B **2**, 2196 (1990)]. After self-focusing, the multi-frequency laser beam inevitably diverges. Remarkably, the longitudinal beatnote compression can compensate the intensity drop due to diffraction. A train of high-intensity radiation spikes with continually evolving longitudinal profile can be self-guided over several Rayleigh lengths in homogeneous plasmas. High amplitude of the EPW is maintained over the entire propagation length. Numerical experiments on the electron acceleration in the cascade-driven (cascade-guided) EPW [using the code WAKE by P. Mora and T. M. Antonsen Jr., Phys. Plasmas **4**, 217 (1997)] show that achieving GeV electron energy is possible under realistic experimental parameters.

Keywords: laser guiding in plasma, self-focusing, relativistic plasma waves, acceleration of electrons by plasma beat wave
PACS: 52.35.-g, 52.35.Hr, 52.35 Mw, 52.38 Hb, 52.38 Kd, 52.65.-y, 52.65.Rr

INTRODUCTION

Two co-propagating laser beams with a difference frequency Ω close to the electron plasma frequency $\omega_{pe} = \sqrt{4\pi e^2 n_0 / m_e}$ (where n_0 is the background electron density, and m_e is the electron rest mass) near-resonantly drive an electron plasma wave (EPW) with a phase velocity close to the laser group velocity in plasma. In a rarefied plasma [$n_0 << n_c$, where $n_c = m_e\omega_0^2/(4\pi^2)$ is a critical plasma density, and ω_0 is the fundamental laser frequency], the EPW phase velocity is close to the speed of light in vacuum. Such a wave can trap relativistic electrons and accelerate them to a high energy [1]. Various recent modifications [2, 3, 4] of the classical plasma beatwave scheme [1] explore possibilities of the EPW excitation using the nonlinearity of the plasma response and manipulations with the laser beat frequency.

In a 3D geometry the plasma beatwave accelerator faces the challenge common for all the laser-based acceleration schemes: the laser diffraction limits the acceleration

CP877, *Advanced Accelerator Concepts: 12th Workshop,*
edited by M. Conde and C. Eyberger

length to roughly a Rayleigh length $Z_R = (\pi/\lambda_0)r_0^2$ (where $\lambda_0 = 2\pi c/\omega_0$ is a laser wavelength, and r_0 is a laser waist radius). In typical experimental conditions Z_R does not exceed few millimeters which strongly limits the electron energy gain. Diffraction is usually suppressed in the experiment by using a plasma channel [5]. In this report we describe an alternative self-consistent method of supporting high laser intensity on axis over few centimeters of *uniform* plasma. We employ a competition between the effects of diffraction (transverse spreading of the beam) and group velocity dispersion (longitudinal compression of radiation beatnotes) [6]. This approach enables guiding of the trains of high-amplitude radiation spikes over several centimeters of plasma while preserving high amplitude of the EPW. Acceleration of electrons to GeV energy appears possible under realistic experimental parameters.

QUASI-GUIDED PROPAGATION OF THE PULSE TRAIN AS A RESULT OF ELECTROMAGNETIC CASCADING

Compressing radiation beatnotes [7] becomes possible due to the increase of laser bandwidth via generation of the coherent cascade of Stokes and anti-Stokes sidebands shifted from the fundamental by integer multiples of the beat frequency Ω [8]. Schematic view of the process is as follows (see Fig. 1). The initially two-frequency pulse is sent into a plasma with a density chosen so as to make ω_{pe} slightly above Ω. Coupling the laser sidebands through the near-resonantly driven EPW generates new sidebands and, eventually, large bandwidth. At the same time, low group velocity dispersion (GVD) does not change significantly the amplitude of the resulting broadband radiation beam. In the next, higher-density, plasma the radiation sidebands are uncoupled, and each of the chirped beatnotes is compressed by the high group velocity dispersion. If the generated bandwidth is close to ω_0, train of single-cycle pulses can be produced.

We have to emphasize that without GVD the nonlinear evolution of laser and plasma results in the laser phase modulation and frequency spectrum broadening only. If the relativistic nonlinearities of laser and plasma wave are neglected, the spectrum of radiation is symmetric with respect to the fundamental, and the number of sidebands on either side is proportional to the product of the propagation length, laser wavelength, and absolute value of the driven electron density perturbation,

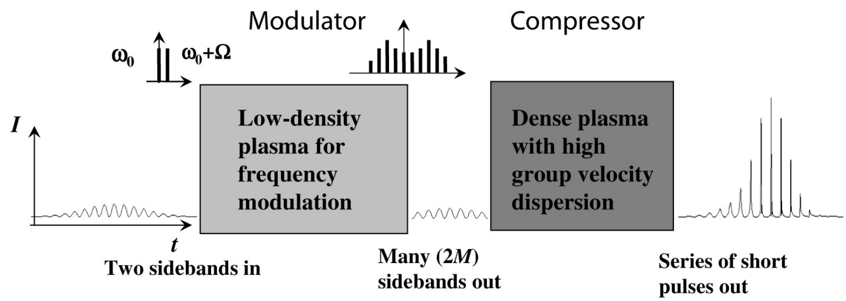

FIGURE 1. Schematic of the two-stage cascade compressor [7]. The frequency modulation (FM) occurs in a rarefied plasma. Denser plasma is used for the compression of beat notes.

$M \sim r_e z \lambda_0 \, |n_e - n_0|$, where $r_e = 2.8 \times 10^{-13}$ cm. The correct sign of the frequency chirp is achieved at $\Omega < \omega_{pe}$; then, near the center of each beatnote, the Stokes (red) sidebands are advanced in time, and the anti-Stokes (blue) ones are retarded. When the GVD is nonzero, the blue sidebands catch up with the red ones near the beatnote center creating an intensity peak.

In reality, the sideband coupling, generation of the bandwidth, and beatnote compression proceed simultaneously in 3D geometry. Relativistic nonlinearities of laser and plasma wave contribute to the increase of bandwidth, and the GVD compresses the beatnotes [7]. Numerous examples of 1D cascade dynamics can be found in Refs. [6, 7]. In a 3D plasma of a real-scale experiment the transverse dynamics of the system is highly important. There may be a competition [6] between the transverse (diffraction) and longitudinal (cascade compression) effects which allows to support high laser intensity near axis over a cm-long propagation length. We explore this guiding opportunity by making a series of numerical experiments via 3D (in cylindrical geometry) time averaged fully relativistic PIC code WAKE [9]. The laser beam propagation is described in the extended paraxial approximation (i.e., the GVD is included). The plasma response is quasistatic. The variables r (radius), z (propagation variable), and $\xi = ct - z$ (retarded time) are used. Evolution of physical quantities is traced from $z = 0$ (laser focal plane) to $z = 3Z_R \approx 3.8$ cm. Two-frequency laser with an envelope $a(r,\xi) - a_0(1 + e^{-i\Omega\xi/c})e^{-\xi^2/(c\tau_L)^2 - r^2/r_0^2}$ is taken as a boundary condition at $z = 0$. At any z, plasma is quiescent, fully ionized, and homogeneous ahead of the pulse (i.e., at $\xi \to -\infty$). The basic set of laser parameters is as follows: $\lambda_0 = 0.8$ μm, $\tau_L \approx 660$ fs, $r_0 \approx 57$ μm, $a_0 = 0.3$ (laser peak intensity $I_{max} \approx 7.8 \times 10^{17}$ W/cm^2). Plasma density is $n_0 = 8.8 \times 10^{17}$ cm^{-3}, so the Lorentz factor associated with the laser group velocity is $\gamma_g = \omega_0/\omega_{pe} \approx 44.6$, and the normalized laser duration and radius are $\omega_{pe}\tau_L \approx 34.75$ and $k_p r_0 = 10$ (where $k_p = \omega_{pe}/c$). The large focal spot implies quasi-1D dynamics of the system (at least, initially). Importantly, the power of either beam is less than one third of the critical one $P_{cr} = 16.2(n_c/n_0)$ GW for the relativistic self-focusing of a single beam [10]. This allows to neglect the

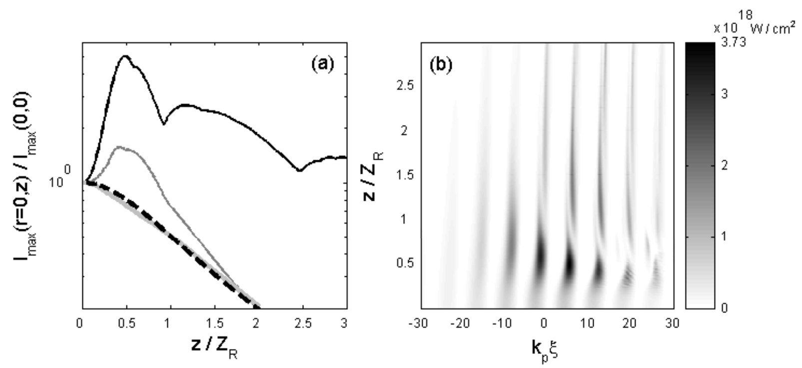

FIGURE 2. (a) The peak normalized laser intensity on axis vs. propagation distance. The reference curve corresponding to the propagation in vacuum is dashed. Other curves are obtained at $\Omega = 1.2\omega_{pe}$ (light gray), $\Omega = \omega_{pe}$ (medium gray), $\Omega = 0.9\omega_{pe}$ (solid black). (b) Laser intensity (in W/cm^2) on axis as a function of propagation distance for $\Omega = 0.9\omega_{pe}$.

relativistic self-focusing of the two-frequency laser [11, 12] and concentrate on the phenomena brought about by the EPW excitation and cascade evolution.

We made a series of simulations with all the laser and plasma parameters fixed except for the value of beat frequency Ω. The peak intensity on axis vs. propagation length is depicted in Fig. 2(a). Figures 2(b) and 3 correspond to the case of $\Omega = 0.9\omega_{pe}$. Figure 2(b) shows the on-axis intensity profile vs. propagation distance. Figure 3 demonstrates the radial-temporal intensity profile and laser frequency spectra in the entrance plane ($z = 0$), in the plane of maximal transverse focusing ($z = 0.5Z_R$), and in the exit plane ($z = 3Z_R$).

The results of modeling show that the laser beams radially diverge, and the intensity on axis drops if $\Omega \geq \omega_{pe}$. On the other hand, at $\Omega < \omega_{pe}$, the laser intensity on axis remains higher than in the focal plane over the entire propagation length. We can identify two distinct regimes of laser evolution in this case. The laser intensity growth at $z \leq 0.5Z_R$ is a consequence of *transverse* compression [see Fig. 3(b)] due to the plasma wave induced self-focusing [12]. There is no longitudinal compression of beatnotes during this stage. At $z > 0.5Z_R$ the multi-frequency radiation beam diverges and the intensity drops. The radiation bandwidth, however, is already quite large [see 3(e)], and the longitudinal/temporal compression of the laser beatnotes begins. The resulting field enhancement balances the drop due to the transverse diffractive spread, and the intensity starts growing again at $z \approx Z_R$ [see Fig. 2]. Notably, the diffraction is not suppressed, and the beam continues to spread out [compare the beam radial sizes in Figs. 3(b) and 3(c)]. During this stage of evolution, high intensity near axis is preserved only at the expense of beatnote temporal shrinkage. This quasi-guiding is observed over 3 Rayleigh lengths. At the end of simulation the beatwave pulse is transformed into a train of nearly flat few-cycle spikes separated in time by the beat period $2\pi/\Omega$ [Fig. 3(c)]. The beatnote compression by a factor of ~ 7 is achieved.

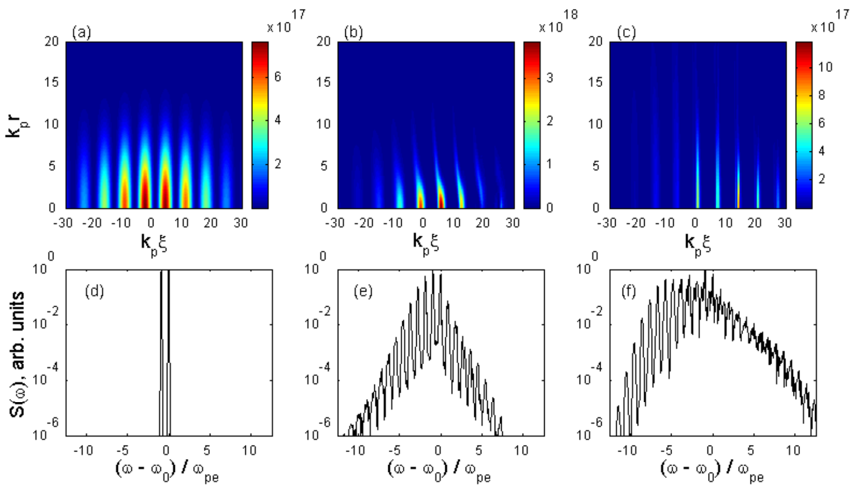

FIGURE 3. Radial and temporal profiles of laser intensity (in W/cm^2) (a-c) and radially integrated laser frequency spectrum (d-f) at (a,d) $z = 0$, (b,e) $z = 0.5Z_R$, (c,f) $z = 3Z_R$ under parameters of Fig. 2(b).

Although the laser beam in this example is several plasma periods long and wide, there is no sign of the transverse distortions due to the near-forward stimulated Raman scattering (SRS) (this instability is not precluded from the numerical scheme [13]). In fact, the presence of long-wavelength EPW ($\lambda_{EPW} \sim 2\pi/k_p$) suppresses the Raman sidescatter [14]. The spectrum of radiation cascade [Fig. 3(f)] is broad (about 25 sidebands) and slightly red-shifted. By the end of simulation, the laser spends about 40% of energy on the EPW excitation. The electron density perturbation in the wave exceeds 30% of n_0 over the entire propagation length, which is promising for the accelerator applications.

The quasi-guiding effect is directly related to the GVD of radiation and thus should be enhanced in denser plasmas. We double the electron density and run the simulation in two different modes. Peak intensities vs. propagation length from these runs are plotted in Fig. 4. The reference set of parameters is that of Figs. 2(b) and 3. First [Fig. 4(a)], we preserve the laser geometry (spot size, duration, beat frequency in physical units) and fix the product a_0n_0. Then, two-fold increase in n_0 leads to the reduction of power by a factor of 4. As a consequence, the ratio of the laser power to the critical power becomes twice smaller. Secondly [Fig. 4(b)], the normalized quantities ($\omega_{pe}\tau_L$, k_pr_0, Ω/ω_{pe}, and a_0) are fixed, and only n_0 is increased. The stage of plasma wave induced self-focusing ($z \leq Z_R$) remains almost unchanged in both cases. Figures 4(a) and 4(b) show that the relative increase in intensity is the same regardless of the plasma density; the normalized duration of the self-focusing stage is also preserved. On the contrary, field enhancement in the quasi-guiding (cascade compression) stage ($z > Z_R$) is more pronounced at the higher density. Interestingly, density increase together with the reduction of laser power results in more pronounced guiding effect [compare gray curves in Figs. 4(a) and (b)]. As far as acceleration of electrons injected into the cascade driven plasma wave is concerned, we should note that, although the guiding effect enhances, both laser beams and EPW slow down in denser plasmas. Therefore, achieving the maximal energy gain requires optimization of the laser and plasma parameters. We shall address this problem in future publications. At this moment we have found that the parameters of Figs. 2 and 3 ($\Omega = 0.9\omega_{pe}$) are sufficient for accelerating the electrons to hundreds of MeV.

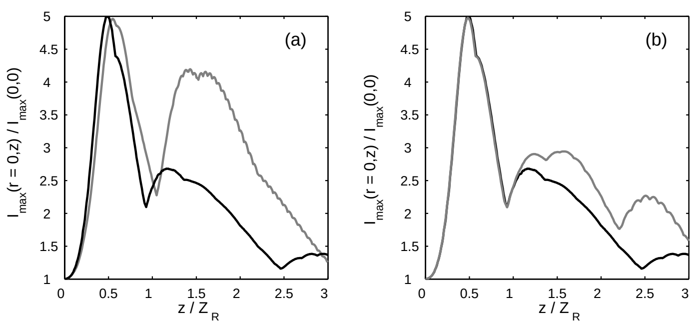

FIGURE 4. The peak normalized laser intensity on axis vs. propagation distance. Solid black curve is exactly the same as that in Fig. 2(a). Gray curves correspond to twice higher electron density. Plot (a): τ_L, r_0, Ω are the same in physical units; product $a_0\, n_0$ is fixed. Plot (b): normalized quantities $\omega_{pe}\tau_L$, k_pr_0, Ω/ω_{pe}, a_0 are fixed. Both plots show enhancement of the guiding effect at higher density.

ELECTRON ACCELERATION IN THE CASCADE-DRIVEN ELECTRON PLASMA WAVE

Preliminary simulations show that strongly nonlinear evolution of the laser beam and plasma wave during the self-focusing stage ($z < Z_R$) preclude the monoenergetic acceleration of electrons injected in the focal plane ($z_{\rm inj} = 0$). On the contrary, during the guided stage ($Z_R \le z \le 3Z_R$) the amplitude and phase velocity of weakly nonlinear EPW vary steadily. This is favorable for reduction of final energy spread of accelerated electron bunches. Hence, we propose to inject electrons *inside a plasma slab* at the beginning of the guided stage ($z_{\rm inj} = 0.85Z_R$). This can be implemented in the laboratory experiment with the help of the all-optical injection scheme using colliding laser pulses [15]. The scheme employs a driving laser and another, short ($< 2\pi/\omega_{pe}$) counter-propagating laser pulse of low intensity. Every time the short pulse crosses with a relativistically intense beatnote of the driving laser the short-wavelength ponderomotive force pushes the background plasma electrons strongly enough to make them trapped in the plasma wave potential bucket immediately behind the given beatnote. As a consequence, the electron injection occurs into several plasma wave periods in the region where the beatwave pulse intensity is high.

To model the injection we uniformly distribute 3×10^4 test electrons in time over 5 plasma wave periods located near the maximum of the beatwave pulse in the injection plane $z_{\rm inj} = 0.85Z_R$. Their initial Lorentz factor is $\gamma_{e0} = 1.1$. The root-mean-square radius of the electron beam is $\sigma_e = 3(c/\omega_{pe}) \approx 17$ μm, and the initial angular spread is zero. The electrons are extracted at $z_{\rm ext} = 3Z_R$ (acceleration length about 2.75 cm). Laser and plasma parameters are those of Fig. 3.

Various characteristics of accelerated electrons at the extraction plane are shown in Fig. 5. Electron energy spectrum [Fig. 5(b)] exhibits several clearly separated peaks (at approximately 415, 600, 750, and 850 MeV) which correspond to acceleration in different plasma wave periods [Fig. 5(a)]. The normalized transverse emittance of the fastest electrons is less than π mm mrad [Fig. 5(c)]. The proposed injection scheme thus allows obtaining several quasi-monoenergetic bunches of few-hundred-MeV electrons with a low transverse emittance in a single laser shot.

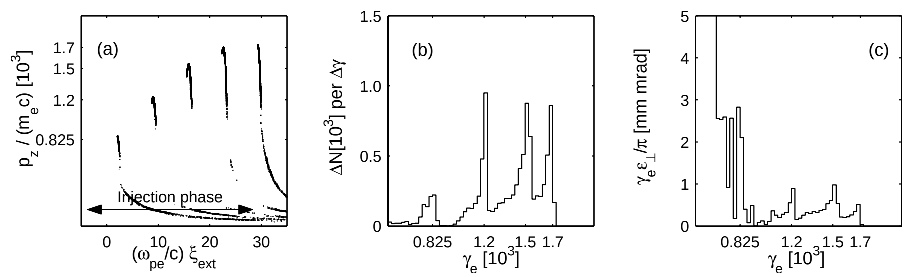

FIGURE 5. (a) Longitudinal phase space, (b) energy spectrum (number of particles per energy spectrometer bin, $\Delta\gamma = 25$), and (c) normalized transverse emittance of test electrons in the extraction plane $z_{\rm ext} = 3Z_R$, $\xi_{\rm ext} \equiv ct - 3Z_R$; 3×10^4 test electrons were injected at $z_{\rm inj} = 0.85Z_R$.

CONCLUSION

The effect of electromagnetic cascading in plasmas can produce trains of few-cycle intense radiation spikes. The electron plasma wave driven by the frequency downshifted ($\Omega < \omega_{pe}$) beatwave chirps the laser frequency, and the group velocity dispersion of radiation compresses the chirped beatnotes. In 3D axi-symmetric geometry, the beatwave-driven frequency downshifted electron density perturbation not only modulates the laser phase, but also causes the radiation beam self-focusing. At the later stage of propagation, compression of the phase-modulated beatnotes compensates the intensity drop due to the diffraction. Thus, the radiation beam can exhibit self-guided propagation over few Rayleigh lengths in a homogeneous plasma. High amplitude of the EPW is maintained over the entire propagation length. Numerical experiments on electron acceleration in the cascade-driven (cascade-guided) EPW promise energy gain of several hundreds MeV in an inch-long plasma without a channel.

ACKNOWLEDGMENTS

The work is supported by the U.S. DOE grants No. DE-FG02-04ER54763 and DE-FG02-04ER41321, and by the NSF grant PHY-0114336 administered by the FOCUS Center at the University of Michigan, Ann Arbor.

REFERENCES

1. T. Tajima and J. M. Dawson, Phys. Rev. Lett **43**, 267 (1979).
2. R. R. Lindberg, A. E. Charman, J. S. Wurtele, and L. Friedland, Phys. Rev. Lett. **93**, 055001 (2004).
3. G. Shvets, Phys. Rev. Lett. **93**, 195004 (2004).
4. O. Polomarov and G. Shvets, Phys. Plasmas **13**, 054502 (2006).
5. S. Ya. Tochitski, R. Narang, C. V. Filip *et al.*, Phys. Plasmas **11**, 2875 (2004); C. V. Filip, R. Narang, S. Ya. Tochitski *et al.*, Phys. Rev. E **69** 026404 (2004).
6. S. Kalmykov and G. Shvets, Phys. Plasmas **13**, 056707 (2006).
7. S. Kalmykov and G. Shvets, Phys. Rev. Lett. **94**, 235001 (2005); Phys. Rev. E **73**, 046403 (2006).
8. B. I. Cohen, A. N. Kaufman, and K. M. Watson, Phys. Rev. Lett. **29**, 581 (1972).
9. P. Mora and T. M. Antonsen Jr., Phys. Plasmas **4**, 217 (1997).
10. G.-Z. Sun *et al.*, Phys. Fluids **30**, 526 (1987).
11. E. Esarey, A. Ting, and P. Sprangle, Appl. Phys. Lett. **53**, 1266 (1988).
12. P. Gibbon, Phys. Fluids B **2**, 2196 (1990).
13. T. M. Antonsen, Jr. and P. Mora, Phys. Fluids B **5**, 1440 (1993).
14. N. E. Andreev and S. Yu. Kalmykov, IEEE Trans. Plasma Sci. **PS-28**, 1106 (2000).
15. G. Fubiani, E. Esarey, C. B. Schroeder, and W. P. Leemans, Phys. Rev. E **70**, 016402 (2004); V. Malka, "GeV laser-plasma accelerators design studies," in this proceedings.